Ferromagnetic properties of epitaxial manganite films on $SrTiO_3$/Si heterostructures

A. K. Pradhan,[a] J. B. Dadson, D. Hunter, K. Zhang, S. Mohanty, E. M. Jackson, B. Lasley-Hunter, K. Lord, T. M. Williams, and R. R. Rakhimov
Center for Materials Research, Norfolk State University, 700 Park Avenue, Norfolk, Virginia 23504

J. Zhang and D. J. Sellmyer
Department of Physics and Astronomy, University of Nebraska, Lincoln, Nebraska 68588-0113 and Center for Materials Research and Analysis, University of Nebraska, Lincoln, Nebraska 68588-0113

K. Inaba and T. Hasegawa
Department of Chemistry, University of Tokyo, 7-3-1 Hongo, Bunkyo-ku, Tokyo 113-0033, Japan

S. Mathews, B. Joseph, and B. R. Sekhar
Institute of Physics, Sachivalaya Marg, Bhubaneswar 751 005, Orissa, India

U. N. Roy, Y. Cui, and A. Burger
Department of Physics, Fisk University, 1000, 17th Avenue North, Nashville, Tennessee 37208

(Received 21 November 2005; accepted 8 June 2006; published online 3 August 2006)

We report on the magnetic properties of epitaxial $La_{0.7}Ba_{0.3}MnO_3$ and $La_{0.7}Sr_{0.3}MnO_3$ films on Si (100) and Si (111) substrates using $SrTiO_3$ template layer, which demonstrate magnetic and electrical properties at and above room temperature. The magnetization data show magnetic transition and magnetic hysteresis at and above room room temperature. The films show well-defined magnetic domains. The ferromagnetic resonance studies show anisotropic effects related to ferromagnetic properties of films. The smaller grain size of about 20 nm in manganite films on $SrTiO_3$/Si may be one of the reasons to minimize the strain effect through strain relaxation at the interface between $SrTiO_3$ and manganites through the formation of three-dimensonal islands.
 [DOI: 10.1063/1.2222402]

I. INTRODUCTION

Since the discovery of colossal magnetoresistance[1,2] (CMR) mixed valence manganites have received a considerable research interest from the scientific community[1–6] owing to their unique properties leading to potential applications in magnetic, magnetoelectronic, photonic devices, infrared detector, as well as spintronic technology. The interplay among the spin, charge, and orbital degrees of freedom in these materials[3–6] leads to many intriguing phenomena, such as metal-insulator transition, magnetic phase transition, and nanoscale electronic phase separation leading to percolative electron transport phenomena in the context of both charge and orbital orderings.[1–9] Although advances have been made in the preparation of nano- and microcrystalline manganites[10–20] on different substrates, films integrated onto Si and other potential semiconductors and their physical investigations have not been possible due to large substrate and film lattice mismatch, mechanical and chemical disaccords arising from the structural dissimilarities. However, the fabrication of either artificial nanostructured or epitaxial films on semiconductors using a template layer could mitigate these problems allowing one to obtain device-quality films.

The perovskite lanthanum-based manganites ($R_{1-x}B_xMnO_3$, where R and B are rare earth and alkaline metals, respectively) films have been successfully grown on single crystal oxide substrates, such as $SrTiO_3$ (STO), $LaAlO_3$ (LAO), and $NdGaO_3$, however, the growth on Si is very limited.[13] In order to integrate an infrared detector (bolometer) array with complementary metal-oxide-semiconductor readout as well as field-effect-transistor (FET) architecture on the same Si wafer CMR materials need to be grown on Si. On the other hand, it can serve as a high-density memory on Si. However, integrating the manganites onto the semiconducting materials, such as on Si, remains a challenging task for potential device applications that utilize both information processing and data storage in the same device. The recent progresses on direct integration[21,22] of STO on Si have opened a possibility to integrate both STO and $R_{1-x}B_xMnO_3$ onto this technologically important semiconductor. On the other hand, it is necessary to grow thinner films of manganites on Si using single ultrathin ($\leqslant$20 nm) template layer for actual technological applications. In the present study, we report the magnetic properties of high-quality epitaxial $La_{0.7}Ba_{0.3}MnO_3$ (LBMO) and $La_{0.7}Sr_{0.3}MnO_3$ (LSMO) films grown by pulsed-laser deposition (PLD) on STO/Si (100/111) heterostructures that demonstrate remarkable ferromagnetic properties in the vicinity of room temperature for eminent device applications.

II. EXPERIMENT

$R_{1-x}B_xMnO_3$, (RBMO)/STO/Si(100/111) films were grown by the PLD technique (KrF excimer, $\lambda = 248$ nm) with a pulse energy density of 1–2 J/cm^2. The films were deposited with a substrate temperature of 700–800 °C, keeping

[a]Electronic mail: apradhan@nsu.edu

the oxygen partial pressure within 200–400 mTorr. X-ray diffraction (XRD) shows that the RBMO films grow epitaxially on STO buffered Si substrates.[23] The STO thickness was limited to only 20 nm. The film thickness and composition inferred from Rutherford backscattering (RBS) using 3 MeV He^{4+} ions at an angle of 160°. The simulation of the RBS spectra was done using GISA 3.9 program[24] assuming respective stoichiometry. The film thickness obtained from the simulated spectra is about 55 nm and this is in good agreement with those obtained by stylus measurements. The simulated results from the RBS spectra give very similar stoichiometry of both STO and manganites used for the target material, elucidating uniform distribution of all elements, especially Mn. The RBS spectra also reveal high crystalline nature without any significant interface diffusion or disorders. The x-ray compositional mappings for Mn in LBMO and LSMO films of STO buffered Si(100) using energy dispersive x-ray analysis fairly show the uniform distribution of Mn on the surface of both films. The atomic force microscopy (AFM) images reveal that the surface is comprised of nanometer (~20 nm) sized grains. The reason for such growth behavior is as follows. The overall growth mode can be considered as Volmer-Weber growth in which the energy relaxation takes place via the formation of three-dimensional (3D) islands to minimize the energy. If the strain energy is large, particularly compressive in nature as in manganites, the system will try to rearrange itself as to find a lower energy state, favoring the formation of 3D islands which may consist of very small grains.

Magnetization (M) and magnetic hysteresis were measured by a superconducting quantum interference device (SQUID) magnetometer with in-plane magnetic field. Electrical transport was studied by a four-probe ac technique. The local magnetic field mapping was done using a scanning SQUID microscopy (SSM). The ferromagnetic resonance (FMR) experiments were done on a Bruker EMX spectrometer operating at 9.6 GHz microwave frequency.

III. RESULTS AND DISCUSSION

The temperature dependence of the magnetization is shown in Fig. 1 for both LBMO and LSMO nanocrystalline films in a field of 0.1 T with the film surface parallel to the applied magnetic field. The magnetic transitions inferred from the zero-field-cooled (ZFC) magnetization for LBMO films grown both on Si(100) and Si(111) are fairly sharp with T_c=315 K as shown in Fig. 1(a). The LBMO films demonstrate ferromagnetic hysteresis at 300 K with a ferromagnetic saturation field of about 4000 G as demonstrated in the inset of Fig. 1(a). Both ZFC and FC magnetizations shown in Fig. 1(b) show the ferromagnetic transition of LSMO with T_c =330 K, which is fairly sharp. They display ferromagnetic hysteresis at room temperature as shown in the inset of Fig. 1(b). The magnetization results clearly show that the magnetic transitions in the above films are enhanced compared to those of previously reported[23] on both LBMO/STO/MgO and LSMO/STO/MgO films. The corresponding zero-field resistivity results are also shown in Figs. 2(a) and 2(b) for both LBMO/STO/Si and LSMO/STO/Si multilayers, respectively. The temperature dependence of resistivity reveals a remarkable sharp jump at the metal-insulator transition temperature (T_{MI}) and is consistent with the magnetic transition.

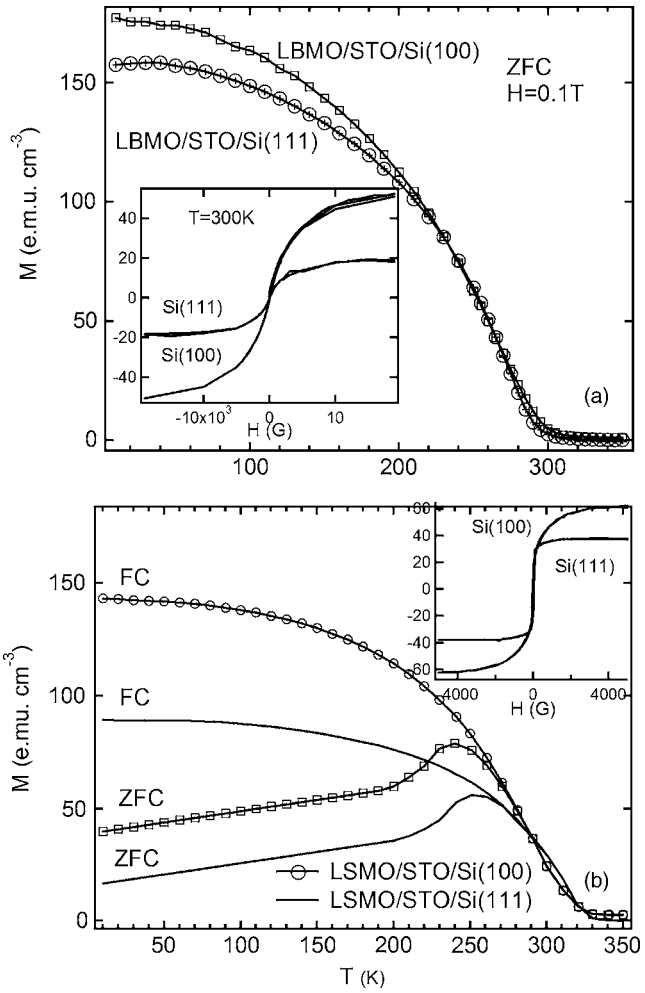

FIG. 1. (a) The temperature dependence of the zero-field-cooled (ZFC) magnetization of LBMO/STO film on Si(100) and Si(111) substrates indicating the transition temperature. (b) The temperature dependence of ZFC and FC magnetizations of LSMO/STO film. The insets show the magnetization hysteresis for both films at room temperature.

In order to map the microscopic magnetic domain structure in these multilayered nanocrystalline films without an external magnetic field, the scanning SQUID magnetic measurements were performed at T=3 K and the images are presented in Figs. 3(a) and 3(b) for LBMO/STO/Si(100) and LBMO/STO Si(111), respectively. The color bar indicates the measured magnetic field B_z perpendicular to the sample surface. Magnetic domains are clearly seen from the images in both samples. The magnetic domains of larger than 30 and 15–20 μm are seen in LBMO/STO/Si(100) and LBMO/STO/Si(111), respectively. These are significantly larger than the length scale of the scenario of electronic phase separation.[4,8] However, the local field intensity is three times larger in LBMO/STO/Si(111) than that of in Si(100), indicating that film of Si(111) generates a more intense field. One of the possible reasons for this is the nature of microscopic difference in grain sizes, assembly, and related strains in the film. On the other hand, local magnetization also depends on the uniaxial anisotropy, most probably arising from magnetostriction.

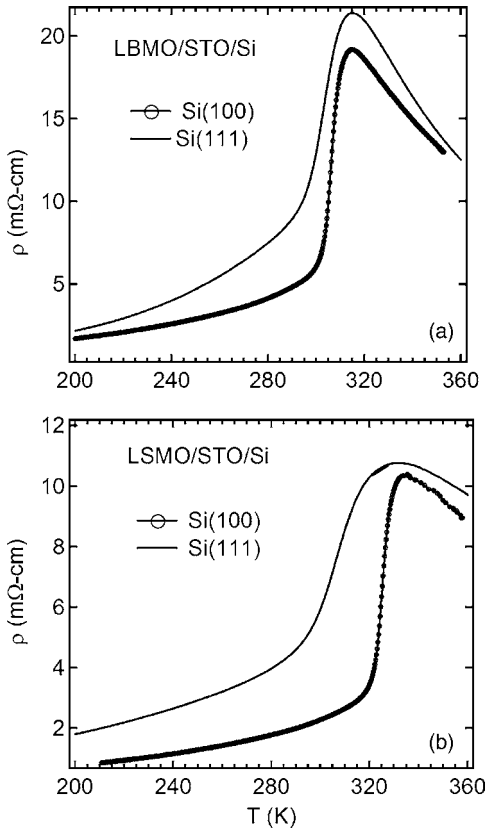

FIG. 2. The electrical resistivity of (a) LBMO and (b) LSMO films on Si(100) and Si(111) substrates.

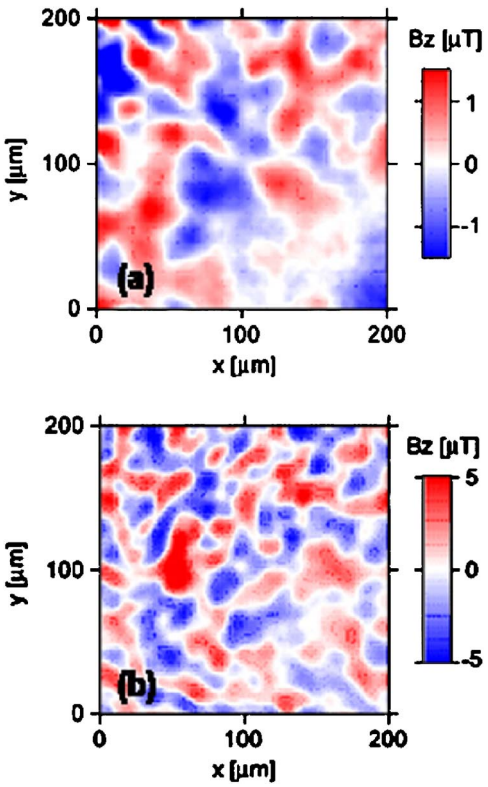

FIG. 3. (Color online) (a) Scanning SQUID microscopic (SSM) image of LBMO/STO/Si(100) film at $T=3$ K, revealing ferromagnetic magnetic domains of about 30 μm in size. (b) The SSM image of LBMO/STO/Si(111) film at $T=3$ K, revealing ferromagnetic magnetic domains of about 10–20 μm in size. The color bars indicate the local magnetic field B_z in the units of microtesla.

FMR studies are probably the most sensitive method for detecting ferromagnetic order as well as the possible existence of other magnetic species. FMR studies were performed on all LBMO and LSMO films and presented in Figs. 4(a) and 4(b). It is remarkable to note that the LBMO films display pronounced ferromagnetic resonance from room temperature down to 100 K. The LSMO films also show FMR up to 325 K. The narrowing of the FMR linewidth for LSMO and LBMO is shown as a function of temperature in the inset of Fig. 4(a). The dip in linewidth of $T=350$ K reflects the crossover from a ferromagnetic state to a paramagnetic state. The FMR linewidth is a sensitive probe for providing magnetic homogeneity in the film.[25,26] The temperature independent and narrower linewidths are the signature of the homogeneous sample. In view of this, the temperature versus linewidth curve for LBMO/STO/Si(100) film is almost independent of temperature, illustrating that the film is fairly magnetically homogeneous. In the case of LBMO/STO/Si, the increase of FMR linewidth, especially at low temperature indicates, presumably, the effects of strains or other disorder in the film. This is consistent with the results[27] of LBMO films directly grown on $LaAlO_3$. However, the present linewidth is slightly larger than the reported value for manganite films grown on *Y*-stabilized zirconia buffered Si substrate using $Bi_4Ti_3O_{12}$ texturing layer.[28] It is noted that in contrast to the present report both buffer and texturing layers reported in Ref. 26 are each 100 nm thick. On the other hand, the manganite layer is also about 100 nm thick. The observed higher T_c and narrower FMR linewidth is due to the complete strain relaxation in such heterostructures. However, the present thinner buffer layer has certainly strain effects which affect the physical properties of the magnanite film which almost half of the thickness of the reported film.[28]

The temperature dependent FMR spectra for LBMO present a characteristic feature centered at about $g=2$ at 300 K and is gradually reduced with decreasing temperature. The films demonstrate FMR signals in which both position and width of the line strongly dependent on the sample orientation, shifting to lower fields at the parallel orientation (magnetic field in the film plane), and to higher fields at the perpendicular orientation. The resonant field positions changing with the angle between the film surface and the applied magnetic field are shown in Fig. 4(b). The inset shows the variation of the resonance field H_θ as the applied field is rotated from the parallel to the perpendicular direction at 300 K. At first sight, the FMR data shows that the films have uniaxial anisotropy. The fitting of the experimental data for LBMO/STO/Si film with a linewidth of <100 G below 300 K with $B_{\text{eff}}=500$ G and $B_a=0$ G at room temperature, $B_{\text{eff}}=2500$ G and $B_a=0$ G at 77 K has been demonstrated in our recent report[29] using a predicted theory.[30] The angular dependence of the FMR signal is a complicated phenomenon, especially in films due to the shape effects. The variation could also arise from other contributions such as

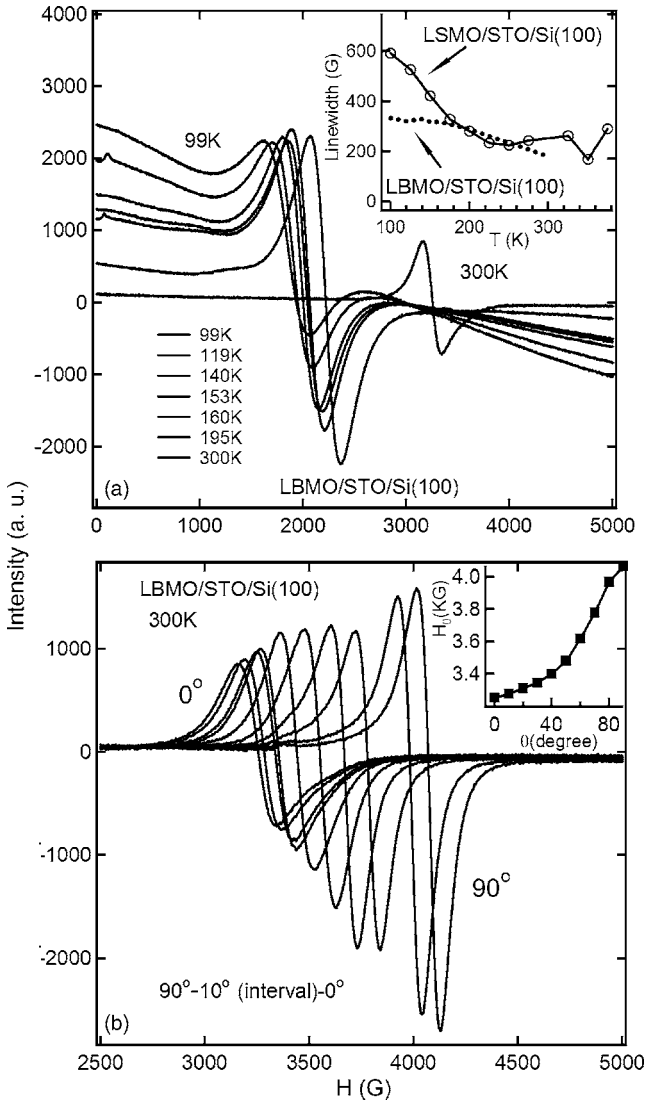

FIG. 4. (a) Ferromagnetic resonance (FMR) spectra of LBMO/STO/Si(111) film at different temperatures. The inset also shows the FMR linewidth for LBMO and LSMO films. (b) The angle dependence of FMR spectra of LBMO film at 300 K, illustrating shifting of the resonant field position with angle. The inset shows resonance field H_θ as a function of angle.

geometric factors and different residual stress in the film as discussed in other reports.[25,26] The detailed studies are necessary in this regard.

The ferromagnetic properties are specifically determined from two factors, the double exchange of electrons between ferromagnetically coupled Mn^{3+} and Mn^{4+} ions and the Jahn-Teller-type electron-phonon interaction due to lattice distortion. The strain effect on T_c and other magnetic and transport properties can be quantified to be a sum of the bulk and Jahn-Teller components. For example, the T_c can be expressed[31,32] as $T_c\ (\varepsilon)=T_c\ (0)(1-\alpha\varepsilon_b-1/2\Delta\varepsilon'^2)$, where ε_b is bulk strain and $\varepsilon'=(1-a/c)$. The decrease in T_c is larger for tensile strain with $\varepsilon_b>0$ than for compressive strain ($\varepsilon_b<0$). The T_c value for LBMO and LSMO films are about 315 and 330 K compared to that of their bulk counterparts with $T_c=340$ and 350 K, respectively. The difference in T_c in films compared to their bulk counterpart is sensitively dependent on the strain developed between the films and the substrates, oxygen concentration, local composition variation, and as well as *A* and *B* site vacancies. However, one of the possible explanations for the enhancement of T_c in films is that the observed grains of 20 nm size in manganite films on STO/Si can minimize the strain effect through strain relaxation at the interface between STO and manganites through the formation of 3D islands as discussed earlier. This will result in the enhancement of both magnetic and metal-insulator transitions in manganite films. Therefore, a great deal of work is necessary to optimize the film growth of manganites on buffered Si substrates.

IV. CONCLUSION

In summary, we have fabricated high-quality epitaxial LBMO and LSMO films on Si (100) and Si (111) substrates using $SrTiO_3$ template layer, which demonstrate remarkable magnetic and electrical properties at and above room temperature. The magnetization data show magnetic transition above room temperature and magnetic hysteresis at room temperature. The films show well-defined magnetic domains. The ferromagnetic resonance studies show anisotropic effects related to ferromagnetic properties of films. The self-organized nanocrystalline manganite films on STO/Si may be one of the reasons to minimize the strain effect through strain relaxation at the interface between STO and manganites through the formation of 3D islands. This will result in enhancement of both magnetic and metal-insulator transitions in manganite films.

ACKNOWLEDGMENTS

This work is supported by the NASA and NSF for Center for Research Excellence in Science and Technology (CREST) Grant No. HRD-9805059. One of the authors (R.R.R.) acknowledges the support from faculty research program provided by NASA. Research at the University of Nebraska is supported by NSF-MRSEC, ONR, and CMRA.

[1] S. Jin, T. H. Tiefel, M. McCormack, R. A. Fastnacht, and R. Ramesh, Science **264**, 413 (1994).
[2] R. von Helmholt, J. Wecker, B. Holszapfel, L. Schultz, and K. Samwer, Phys. Rev. Lett. **71**, 2331 (1993).
[3] A. Moreo, S. Yunoki, and E. Dagotto, Science **283**, 2034 (1999).
[4] M. Uehara, S. Mori, C. H. Chen, and S.-W. Cheong, Nature (London) **399**, 560 (1999).
[5] A. J. Millis, Nature (London) **392**, 147 (1998).
[6] Y. Tokura and N. Nagosa, Science **288**, 462 (2000).
[7] M. B. Salamon and M. Jaime, Rev. Mod. Phys. **73**, 583 (2001).
[8] M. Fath, S. Freisem, A. A. Menovsky, Y. Tomoika, J. Aarts, and J. A. Mydosh, Science **285**, 1540 (1999).
[9] J. C. London, N. D. Mathur, and P. A. Midgley, Nature (London) **420**, 797 (2002).
[10] P. Yang, T. Deng, D. Zhao, P. Feng, D. Pine, B. F. Chmelka, G. M. Whitesides, and G. D. Stucky, Science **282**, 2244 (1998).
[11] D. Zhu, H. Zhu, and Y. Zhang, Appl. Phys. Lett. **80**, 1634 (2002).
[12] J. J. Urban, L. Ouyang, M.-H. Jo, D. S. Wang, and H. Park, Nano Lett. **4**, 1547 (2004).
[13] J.-H. Kim, S. I. Khartsev, and M. Grishin, Appl. Phys. Lett. **82**, 4295 (2003).
[14] T. Zhao, S. B. Ogale, S. R. Shinde, R. Ramesh, R. Droopad, Z. Yu, K. Eisenbeiser, and A. Misewich, Appl. Phys. Lett. **84**, 750 (2004).
[15] F. Tsui, M. C. Smoak, T. K. Nath, and C. B. Eom, Appl. Phys. Lett. **76**, 2421 (2000).
[16] Y. Ogimoto, M. Izumi, T. Manako, T. Kimura, Y. Tomioka, M. Kawasaki, and Y. Tokura, Appl. Phys. Lett. **78**, 3505 (2001).

[17]E. R. Buzin, W. Prellier, Ch. Simon, S. Mercone, B. Mercey, B. Raveau, J. Sebek, and J. Hejtmanek, Appl. Phys. Lett. **79**, 647 (2001).
[18]J. Zhang, H. Tanaka, T. Kanki, J.-H. Choi, and T. Kawai, Phys. Rev. B **64**, 184404 (2001).
[19]A. K. Pradhan, D. Sahu, B. K. Roul, and Y. Feng, Appl. Phys. Lett. **81**, 3597 (2002).
[20]A. K. Pradhan, D. Sahu, B. K. Roul, and Y. Feng, J. Appl. Phys. **96**, 1170 (2004).
[21]Z. Yu *et al.*, J. Vac. Sci. Technol. B **18**, 1653 (2000).
[22]Y. Wang *et al.*, Appl. Phys. Lett. **80**, 97 (2002).
[23]A. K. Pradhan *et al.*, Appl. Phys. Lett. **86**, 012503 (2005).
[24]J. Saarilahti and E. Rauhala, Nucl. Instrum. Methods Phys. Res. B **64**, 734 (1992).
[25]S. E. Lofland, S. M. Bhagat, H. L. Ju, G. C. Xiong, T. Venkatesan, and R. L. Greene, Phys. Rev. B **52**, 15058 (1995).
[26]S. M. Bhagat, *ASTM Handbook* (Interscience, New York, 1986), Vol. 10, p. 267.
[27]S. E. Lofland, S. M. Bhagat, H. L. Ju, G. C. Xiong, T. Venkatesan, R. L. Greene, and S. Tyagi, J. Appl. Phys. **79**, 5166 (1996); S. E. Lofland, S. M. Bhagat, C. Kwon, M. C. Robson, R. P. Sharma, R. Ramesh, and T. Venkatesan, Phys. Lett. A **209**, 246 (1995).
[28]Z. Trajonvic *et al.*, Appl. Phys. Lett. **69**, 1005 (1996).
[29]R. Bah, D. Bitok, R. R. Rakhimov, M. M. Noginov, A. K. Pradhan, and N. Noginova, J. Appl. Phys. **99**, 08Q312 (2006).
[30]V. P. Dyakonov, V. Shapovalov, and E. Zubov, J. Appl. Phys. **93**, 2100 (2003).
[31]A. J. Millis, T. Darling, and A. Migliori, J. Appl. Phys. **83**, 1588 (1998).
[32]H. S. Wang, E. Wertz, Y. F. Hu, Q. Li, and D. G. Schlom, J. Appl. Phys. **87**, 7409 (2000).